B7 - 6

10 MV x-ray Scatter Dose Spread Kernel Based on the Bjärngard Scatter Factor (SF) Formalism

Akira Iwasaki
School of Allied Medical Sciences, Hirosaki University,
66-1 Hon-cho, Hirosaki, Aomori 036-8564, Japan

1. INTRODUCTION

Let TMR(z,0) denote the zero-area tissue-maximum ratio (TMR) in water at a depth z on the beam axis and let SMR(z,r) denote the scatter-maximum ratio (SMR) in water at a depth z on the beam axis for a field radius of r. Using the TMR(z,0) and SMR(z,r) functions, the scatter factor (SF) in water for z and r can be expressed as

$$\mathrm{SF}(z,r)=1 + \mathrm{SMR}(z,r)/\mathrm{TMR}(z,0). \tag{1}$$

Bjärngard and his colleagues have proposed an expression for evaluating the SF. It is given by

$$\mathrm{SF}(z,r)=1 + \frac{a_0 \cdot z \cdot r/0.561}{w_0 \cdot r/0.561 + z} \tag{2}$$

where a_0 and w_0 are constants. Let the attenuation coefficient along the beam axis be expressed as $\mu(z)$. Then these constants become $a_0=\mu(0)$ and $w_0=1.73-17.1\mu(0)$, where z and r are expressed in cm, a_0 and $\mu(0)$ are in cm^{-1}, and w_0 is dimensionless. Equation (2) has been constructed under conditions of lateral and longitudinal electron equilibrium. Actually, Eq.(2) leads to SF(z,r)=1 for z=0 for any value of r. Therefore, it can be understood that Eq.(2) is unreasonable at least at depths near z=0.

Let $K_1(\xi,r)$ and $K_2(\eta,r)$ denote the forward and backward scatter dose spread functions in water, respectively (Fig.1). We have

$$K_1(\xi,r)=[\partial^2\mathrm{SMR}(\xi,r)/\partial\xi\,\partial r + \bar{\mu}\,\partial\mathrm{SMR}(\xi,r)/\partial r]/(2\pi\, rK_0) \tag{3}$$

$$K_2(\eta,r)=[\exp(\bar{\mu}\,\eta)\,\partial^2\mathrm{BSR}(\eta,r)/\partial\eta\,\partial r]/(2\pi\, rK_0) \tag{4}$$

where $\bar{\mu}$ is the average attenuation coefficient in water for the beam-axis primary radiation. K_0 is defined as the incident primary water collision kerma at a point in air on the beam axis, divided by the peak primary absorbed dose at the same point in water. It should be noted that all the primary absorbed dose components used in this paper are under conditions of lateral electronic equilibrium.

For 10 MV x rays, we will develop a method of obtaining reasonable SF data in regions of lateral and/or longitudinal electron disequilibrium and then produce a scatter dose spread

kernel using the $K_1(\xi, r)$ and $K_2(\eta, r)$ functions with reasonable SMR data.

2. METHODS

A. The zero-area TMR

As a 10 MV x-ray zero-area TMR expression, we utilize

$$\mathrm{TMR}(z,0)=T_0\exp[-\mu(z)z]-(T_0-C_0)\exp(-az)+U_0\exp(-bz) \tag{5}$$

$$\mu(z)=0.0169\exp(-0.00549z) + 0.0222 \tag{6}$$

where $T_0=1.14838$, $C_0=-100$, $U_0=100.02935$, $a=1.28013$ cm^{-1}, and $b=1.27999$ cm^{-1}. The depth of peak primary absorbed dose is $z_{peak}=2.779$ cm [$d\mathrm{TMR}(z,0)/dz=0$ for $z=z_{peak}$]. We use $\bar{\mu}=0.0365$ cm^{-1}, obtained for depths of $z=0-30$ cm. We use $K_0=1.11678$. It can be proved that the incident water collision kerma of $K_0=1.11678$ can produce the same primary absorbed dose component as expressed by Eq.(5). Using $\mu(0)=0.0391$ cm^{-1}, we can derive $a_0=0.0391$ cm^{-1} and $w_0=1.061$ (Eq.(2)).

B. SMR's at small depths

Let z_0 be a certain value of z above which Eq.(2) can be held reasonably. From Eqs.(1) and (2), for $z \geqq z_0$ we can then derive

$$\mathrm{SMR}(z,r)=\frac{a_0\cdot z\cdot r/0.561}{w_0\cdot r/0.561+z}\mathrm{TMR}(z,0). \tag{7}$$

For $z<z_0$, we propose

$$\mathrm{SMR}(z,r)=\frac{a_0\cdot g(z)\cdot r/0.561}{w_0\cdot r/0.561+g(z)}\mathrm{TMR}(z,0) \tag{8}$$

$$g(z)=f_1\exp(f_2 z) \tag{9}$$

where f_1 and f_2 are constants. The values of the constants are determined as $f_2=1/z_0$ and $f_1=z_0\exp(-f_2 z_0)$. Then we can have $\mathrm{SF}(0,r)>1$ for any non-zero value of r.

C. SMR's at small fields

Let r_0 be a certain value of r above which Eqs.(7) and (8) can be held reasonably. The SMR for small field radii of $r<r_0$ can then be expressed as

$$\mathrm{SMR}(z,r)=F_1(z)r^2 + F_2(z)r^3. \tag{10}$$

3. RESULTS AND CONCLUSIONS

A. The r_0 and z_0 values

We also introduce another function $K_1(t,\theta)$, reconstructed using variations of $t=\sqrt{(\xi^2+r^2)}$ and $\theta=\tan^{-1}(r/\xi)$ for $K_1(\xi,r)$. In order

to determine the values of r_0 and z_0, we set the following four restrictions.

(a) Restriction 1: The SMR(z,r)/TMR(z,0) curve for any non-zero r value should increase with increasing z (refer to Fig.4).

(b) Restriction 2: The $K_1(t,0)$ curve should decrease with increasing t.

(c) Restriction 3: The relation $K_1(t,\theta_1) > K_1(t,\theta_2)$ for $\theta_1 < \theta_2$ should be obtained for any non-zero value of t.

(d) Restriction 4: The values of $K_2(\eta,r)$ should be zero or positive for any values of η and r.

It has been found that the restriction 1 can be satisfied for any values of r_0 and z_0 and that all the four restrictions can not be satisfied in any common region. Neglecting the restriction 4, we finally employed r_0=0.615 cm and z_0=1.055 cm (Fig.2).

B. Scatter dose spread kernels

Figure 3 shows a set of $K_1(\xi,r)$ and $K_2(\eta,r)$ isolines. Both $K_1(\xi,r)$ and $K_2(\eta,r)$ functions take the same maximum value of 0.0316 cm^{-3} at the origins. It can be seen from Fig.3 that the $K_2(\eta,r)$ contribution is very small compared with Monte Carlo generated kernels and that the $K_1(\xi,r)$ isolines show a little unnatural patterns in the region of ξ <1.055 cm (=z_0). The tail-like patterns that the $K_1(\xi,r)$ isolines with 0.74E-04 cm^{-3} and less exhibit in the region of small r and large ξ values are reasonable. Figure 4 shows a set of SMR(z,s)/TMR(z,0) curves, yielded using r_0=0.615 cm, z_0=1.055 cm, and $s=r/0.561$ (s is the square field side). It can be seen that each SMR(z,s)/TMR(z,0) curve is a continuously increasing function with depth z.

We produced another kind of scatter dose spread kernel, where we used the same parameters as used when producing the kernel of Fig.3; however, we let the value of r_0 be a function of ξ, as

$$r_0(\xi)=0.140\xi + 0.615. \tag{11}$$

where r_0 and ξ are expressed in cm. Figure 5 illustrates the result. Figure 6 shows a set of SMR(z,s)/TMR(z,0) curves, yielded using z_0=1.055 cm and Eq.(11) as r_0.

On comparing the two types of scatter dose spread kernels shown in Figs.3 and 5, it can be seen that the kernel of Fig.5 is more similar in shape to the kernels produced using Monte Carlo simulations. The Monte Carlo kernels reported so far do not exhibit such tail-like patterns as Fig.3 does. The SMR(z,s)/TMR(z,0) curves at small fields are not continuously increasing functions with depth z; namely, they are not reasonable. Therefore, it can be understood that such tail-like patterns as shown in Fig.3 certainly have an important role.

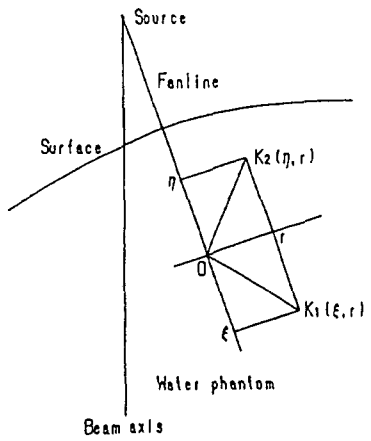

Fig.1. Schematic diagram showing how to use the $K1$ and $K2$ functions.

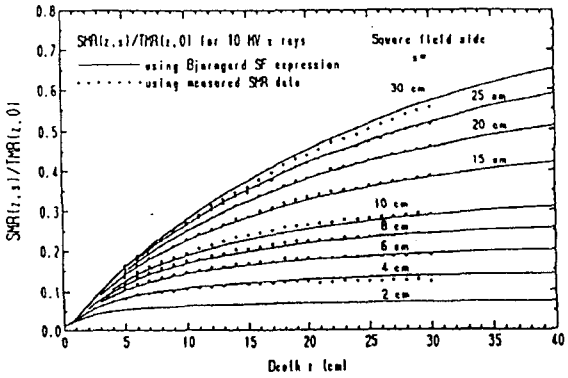

Fig.4. Two sets of SMR(z,s)/TMR(z,0) data for 10 MV x rays. The solid lines were drawn using $z0$=1.055 cm and $s0$=1.096 cm (=$r0$/0.561). The plot marks were yielded using measured SMR data.

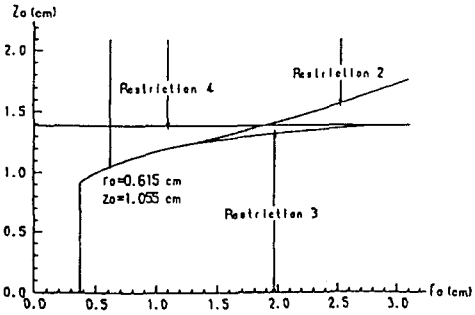

Fig.2. Diagram showing the regions of $r0$ and $z0$ values satisfying the restrictions 2-4. The restriction 1 is satisfied for any values of $r0$ and $z0$. A pair of values of $r0$=0.615 cm and $z0$=1.055 cm has been employed.

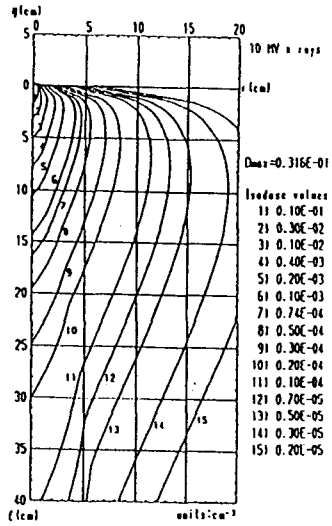

Fig.5. 10 MV x-ray scatter dose spread kernel in water, obtained using the $K1$ and $K2$ functions with $z0$=1.055 cm and Eq.(11) as $r0$.

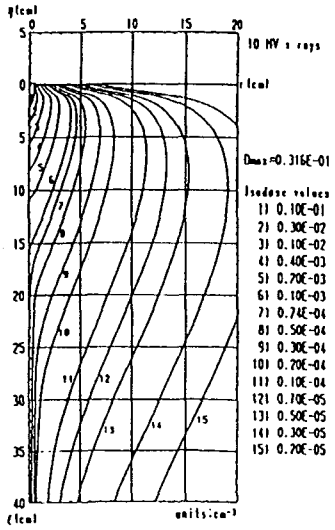

Fig.3. 10 MV x-ray scatter dose spread kernel in water, obtained using the $K1$ and $K2$ functions with $z0$=1.055 cm and $r0$=0.615 cm.

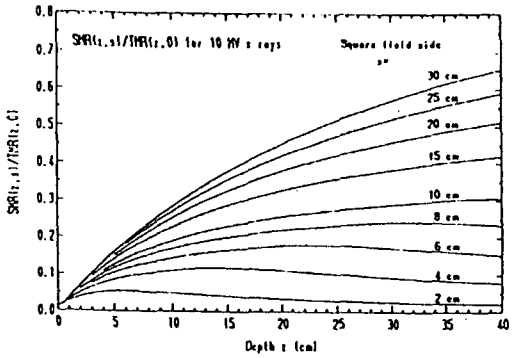

Fig.6. A set of SMR(z,s)/TMR(z,0) curves for 10 MV x rays, drawn using $z0$=1.055 cm and $s0$(z) =$r0$(z)/0.561 (cm).